

Metformin Attenuates Silica-induced Pulmonary Fibrosis via AMPK Signaling

Demin Cheng

Nanjing Medical University

Qi Xu

Nanjing Medical University

Yue Wang

Nanjing Medical University

Guanru Li

Nanjing Medical University

Wenqing Sun

Nanjing Medical University

Dongyu Ma

Nanjing Medical University

Siyun Zhou

Nanjing Medical University

Yi Liu

Nanjing Medical University

Han Lei

Nanjing Medical University

Chunhui Ni (✉ chninjm@126.com)

Nanjing Medical University <https://orcid.org/0000-0002-6539-2434>

Research Article

Keywords: occupational pulmonary fibrosis, metformin, epithelial-mesenchymal transition, fibroblast-myofibroblast transition

Posted Date: June 23rd, 2021

DOI: <https://doi.org/10.21203/rs.3.rs-636285/v1>

License: © ⓘ This work is licensed under a Creative Commons Attribution 4.0 International License.

[Read Full License](#)

Version of Record: A version of this preprint was published at Journal of Translational Medicine on August 16th, 2021. See the published version at <https://doi.org/10.1186/s12967-021-03036-5>.

Abstract

Background: Silicosis is one of the most common occupational pulmonary fibrosis caused by respirable silica-based particle exposure, with no ideal drugs at present. Metformin, a commonly used biguanide antidiabetic agent, could activate AMP-activated protein kinase (AMPK) to exert its pharmacological action. Therefore, we sought to investigate the role of metformin in silica-induced lung fibrosis.

Methods: The anti-fibrotic role of metformin was assessed in 50 mg/kg silica-induced lung fibrosis model. SiO₂-stimulated lung epithelial cells/macrophages and TGF-β-induced differentiated lung fibroblasts were used for in vitro models.

Results: At the concentration of 300 mg/kg in the mouse model, metformin significantly reduced lung inflammation and fibrosis in SiO₂-instilled mice at the early and late fibrotic stages. Besides, metformin (range 2mM to 10mM) reversed SiO₂-induced cell toxicity, oxidative stress, and epithelial-mesenchymal transition process in epithelial cells (A549 and HBE), inhibited inflammation response in macrophages (THP-1), and alleviated TGF-β1-stimulated fibroblast activation in lung fibroblasts (MRC-5) via an AMPK-dependent pathway.

Conclusions: In this study, we identified that metformin might be a potential drug for silicosis treatment.

Introduction

Silicosis is one of the most common occupational pneumoconiosis directly caused by exposure to respirable silica-based particles, which leads to an inflammatory cascade, progressive lung fibrosis, and then devastated respiratory failure[1]. Persistent inflammation, epithelial-mesenchymal transition (EMT), fibroblast proliferation and activation, and extracellular matrix (ECM) excessive deposition contribute to the development of silicosis[2]. Although efforts to improve the work environment have been made for years, the incidence and prevalence of silicosis worldwide have been rising, especially in developing countries like China[3, 4]. However, the underlying pathogenesis of silicosis is still not elucidated and none of the effective therapies can halt disease progression or reverse established lung fibrosis. There is yet an urgent need for developing efficient methods.

Over the past decades, mounting evidence indicates that several pathogenic mechanisms are known to be involved in the progression of silicosis[5]. Multiple studies have identified that a variety of cells include epithelial cells, macrophages, and pulmonary fibroblasts, are participating in the process of silica-induced pulmonary fibrosis[6, 7]. Epithelial-mesenchymal transition (EMT) entails the phenotypic changes and molecular reprogramming which characterize the conversion of epithelial cells to mesenchymal cells[8]. The current notion suggested that epithelial cells participated in the activation and accumulation of myofibroblasts via the EMT process[9]. EMT cells can activate transcription factors, secrete pro-fibrotic cell surface proteins and cytokines, and increase ECM accumulation[10]. Macrophages usually appear pro-inflammatory phenotype at the early stage after exposure to silica and turn to pro-reparative phenotype to facilitate tissue wound healing[11]. Macrophages play a crucial role in the progression of

pulmonary fibrosis by triggering the inflammation cascade response and differentiating into a profibrotic phenotype[12, 13]. Persistent inflammation creates a microenvironment that promotes adaptive immunity, proliferation and migration of fibroblast, secretion of extracellular matrix and deposition of collagen, eventually leading to abnormal lung tissue remodeling and obstructive air exchange, even death[14, 15]. The fibroblast to myofibroblast transition is the hallmark of fibrotic diseases, leading to excessive synthesis and deposition of ECM like Collagen, Fibronectin and Elastin[16, 17]. Thus, suppression of EMT process, inflammatory cascade response and fibroblast activation represents a visible approach for the amelioration of pulmonary fibrosis.

Metformin is a common treatment choice for type 2 diabetes mellitus (T2DM), yet its specific mechanism of utility remains unclear[18]. Numerous studies demonstrated that metformin stimulated AMP-activated protein kinase (AMPK), a key regulator of energy metabolism and balance[19, 20]. In several experimental animal models, apart from T2DM, metformin was found to have other potential effects. Metformin has been acted in other pathologies like cancer, non-alcoholic fatty liver disease, asthma, heart failure, obesity, fibrotic diseases, etc., with varying degrees of effect[21-25]. It is interesting to note that metformin exerts protective effects in various lung diseases by inhibiting inflammation, attenuating oxidative stress, and altering fibroblast-to-myofibroblast transition[26, 27]. Moreover, it has been reported that metformin could reverse established pulmonary fibrosis in the bleomycin-induced mouse lung fibrosis model[28] and low prevalence of pneumoconiosis in diabetic coal-miners[29]. Given this, it appears that metformin can attenuate the key factors leading to fibrosis. Hence, we considered that metformin might be useful in silica-induced pulmonary fibrosis both in vivo and vitro.

In this study, we evaluated the anti-fibrotic effects of metformin in the silica-induced lung fibrosis model at different stages to illustrate the underlying mechanisms in different cell types, including pulmonary epithelial cells, macrophages, and fibroblasts. Functionally, we demonstrated the evidence that metformin did ameliorate the cell toxicity, inflammation, epithelial-mesenchymal transition, and oxidative stress caused by silica and fibroblast activation induced by TGF- β 1. Collectively, metformin may have the therapeutic potential for ameliorating established lung fibrosis.

Material And Methods

Metformin treatment mouse model of the late fibrotic stage

A total of 24 mice were randomly divided into 4 groups (n=6 each group): a saline group, a silica group, a 100 mg/kg of metformin plus silica group, and a 300 mg/kg of metformin plus silica group. All the mice in the silica groups were received a single intratracheal instillation with 50 mg/kg of silica particles (Sigma-Aldrich, St. Louis, MO, USA) dissolved in 0.05 ml sterile saline. After silica treatment for 28 days, the mice of metformin treatment groups were given a corresponding dose of metformin (started from the 28th day, Beyotime Institute of Biotechnology, Shanghai, China) via intragastrical administration daily for two weeks. Then the mice were sacrificed after installation, and the lung tissues were isolated and stored at -80°C for further analysis.

Metformin treatment mouse model of the early fibrotic stage

Another 24 mice were subdivided into 4 groups (n=6 each group): saline, silica, silica plus saline, and silica plus metformin (300 mg/kg, intragastrical administration for 28 days). The method of silica treatment was the same as mentioned above. The silica plus saline and silica plus metformin group were treated via intragastrical administration daily after silica treatment the next day. The mice were sacrificed after the installation treatment for 4 weeks, and the lung tissues were harvested and stored as previously described.

Histopathology

The mouse lung tissues were harvested, fixed with formalin solution overnight and embedded in paraffin. Then the tissues sections (5 μ m) were subsequently stained with hematoxylin and eosin (H&E) to assess fibrosis. To evaluate the pathological changes of the lung tissues, a scoring system was used as previously described[30], lesion severity: 0 = zero/nothing, 1 = marginal, 2 = slight, 3 = moderate, 4 = severe, 5 = very severe; lesion distribution: 0 = absent, 1 = rare/occasional (10% of the lung area), 2 = spares/limited (10%-25% of the lung area), 3 = moderate (25%-50% of the lung area), 4 = extensive/widespread (50%-75% of the lung area), 5 = very extensive/predominant (over 75% of the lung area).

Hydroxyproline content assay

The amounts of collagen in the lung tissues were determined by the hydroxyproline content assay (A030-2, Jiancheng Bioengineering Institute, Nanjing, China). According to the manufacturer's protocol, the amount of collagen was determined by the spectrophotometer at 550 nm and expressed as micrograms per mg of lung tissues.

Cell culture and treatment

The lung epithelial cells (A549 and HBE), lung fibroblast (MRC-5), and the human monocytic cell (THP-1) were commercially obtained from the American Type Culture Collection (ATCC, Manassas, VA, USA). A549 and THP-1 cells were maintained in RPMI Medium 1640 basic (1640, Life Technologies/Gibco, Grand Island, NY, USA), the HBE cells were maintained in Dulbecco's modified Eagle's medium (DMEM, 1640, Life Technologies/Gibco, Grand Island, NY, USA), and the MRC-5 cells were maintained in Minimum Essential Medium (MEM, Life Technologies/Gibco, Grand Island, NY, USA). All of the culture media were containing 10% fetal bovine serum (BISH1475, Biological Industries) and antibiotics (penicillin and streptomycin, Life Technologies/Gibco, Gaithersburg, MD). Cells were cultured at 37°C in a 5% CO₂ atmosphere.

PMA (Sigma–Aldrich) was used to treat THP-1 cells into macrophages. For all the experiments analysis, epithelial cells and THP-1 were treated with 200 or 150 μ g/ml SiO₂ (Sigma-Aldrich, St. Louis, MO, USA) together with various concentration (2, 5, 10 mM) of metformin (Beyotime Institute of Biotechnology, Shanghai, China); MRC-5 cells were treated with 5 ng/ml TGF- β 1 (Sigma-Aldrich) together with metformin.

Cell viability assay

Cell viability was detected with a Cell Counting Kit-8 assay (CCK8, Beyotime Institute of Biotechnology, Shanghai, China) according to the manufacturer's instructions. The cells were plated in a 96-well plate, followed by exposure to different concentrations (0, 50, 100, 150 and 200 µg/ml) of silica and (2 mM, 5 mM and 10 mM) of metformin for the indicated times. Then 10 µl CCK8 reagents were diluted in each well for 1 h at 37°C in 5% CO₂, and the 96-well plate was measured at 450 nm carried out with a microplate reader (TECAN Infinite M200, Mannedorf, Switzerland). The percent viability of the cells was calculated by the formula: cells viability (%) = (A_{450nm}-A_{650nm}) treated/(A_{450nm}-A_{650nm}) control × 100%.

Immunostaining assay

After the indicated treatment, A549 or HBE cells were washed fixed with 4% methanol for 30 min, then stained with anti-Vimentin or anti-E-cadherin antibody (Abcam, ab92547, 1:1000; Cell Signaling Technology, 24E10, 1:1000) at 4°C overnight and incubated with Cy3-conjugated or FITC-conjugated goat anti-rabbit antibody (1:200, Beyotime Institute of Biotechnology, Shanghai, China) for 1h. The DAPI was used to stain the nucleus in cells for 10 min. All the images were acquired with the fluorescence microscope (Olympus, Tokyo, Japan).

Western blot and antibodies

For western blot assay, all cells were washed twice times with PBS and then used with RIPA lysis buffer and phenylmethylsulfonyl fluoride for extraction of total proteins (Beyotime Institute of Biotechnology, Shanghai, China; PMSF, Sigma-Aldrich, St. Louis, MO, USA). The total protein of the tissues was extracted with T-PER Tissue Protein Extraction Reagent (Thermo Scientific). Protein concentrations were measured by BCA Protein Assay (Beyotime Institute of Biotechnology, Shanghai, China). A total of 80 µg of protein extracts were separated via SDS-PAGE and transferred onto polyvinylidene difluoride (PVDF) membranes (ISEQ00010, 0.2 µm, Immobilon). Then the membranes were incubated overnight at 4°C with appropriate primary antibodies and appropriate secondary antibodies. Protein bands were visualized using the ChemiDocXRS + imaging system (Bio-Rad Laboratories, Inc). Densitometry analyses were performed using Image J software.

Primary antibodies are as follows: anti-Fibronectin (Abcam, ab45688, 1:1000); anti-Collagen I (Abcam, ab34710, 1:1000); anti-E-cadherin (Cell Signaling, 24E10, 1:1000); anti-Vimentin (Abcam, ab92547, 1:1000); anti-αSMA (Abcam, ab32575, 1:1000) and anti-GAPDH (Cell Signaling, 13E5, 1:1000).

Wound-healing assay

Cells were seeded in 6-well plates and cultured until the cells reached 70%-80% confluence. Wounds were scratching with a sterile 10 µl pipette tip across the monolayered cells to create a straight linear scratch, and a wound gap was performed by a microscope. After indicated treatment, the widths of the wound

were followed by the previously described procedure. The wound gap was quantitatively evaluated with Image J software.

Quantitative RT-PCR (qRT-PCR)

Total RNA from collected tissues or cells was extracted using the Trizol method as previously described[7]. RNA quality and concentration were measured by Nanodrop 2000 spectrophotometer (ND-100, Thermo, Waltham, MA). All mRNA was detected using AceQ qPCR SYBR Green Master Mix (Vazyme Biotech Co, Nanjing, China) in the ABI 7900HT Real-Time PCR system (Applied Biosystems). Fold changes in the expression levels were calculated using the $2^{-\Delta\Delta Ct}$ method and normalized using GAPDH as the endogenous control.

Reactive oxygen species assay

The intracellular reactive oxygen species (ROS) level was measured by ROS Assay Kit (Beyotime Institute of Biotechnology, Shanghai, China), using an oxidation-sensitive fluorescent probe DCFH-DA according to the manufacturer's instructions. The intensity of fluorescent staining was quantified with Image J software.

Lipid peroxidation assay

The lipid peroxidation product MDA concentration in cell lysates was measured using a Lipid Peroxidation MDA Assay Kit (Beyotime Institute of Biotechnology, Shanghai, China) according to the manufacturer's instructions.

Glutathione assay

The relative GSH concentration in cell lysates was measured using a Total Glutathione Assay Kit (Beyotime Institute of Biotechnology, Shanghai, China) according to the manufacturer's instructions.

JC-1 staining

JC-1 fluorescent probe was employed to measure the mitochondrial depolarization in cells. The mitochondrial membrane potential of cells using a mitochondrial membrane potential assay kit with JC-1 (Beyotime Institute of Biotechnology, Shanghai, China) according to the manufacturer's instructions. Cell treated with CCCP (mainly cause loss of mitochondrial membrane potential) was used as a positive control.

LDH Release Assay

The cell of cytotoxicity was measured by the LDH activity in the supernatant using an LDH Cytotoxicity Assay Kit (Beyotime Institute of Biotechnology, Shanghai, China) according to the manufacturer's instructions.

Statistical analysis

All experiments were performed in triplicates. Statistical analysis was performed using Student's t-test (between two groups) or one-way analyses of variance followed by Tukey's multiple comparisons test (more than two groups). Data were expressed as mean \pm SD. $P \leq 0.05$ was considered statistically significant.

Results

Metformin attenuates SiO₂-induced lung fibrosis in vivo.

To elucidate whether metformin has a potential role in silica-induced pulmonary fibrosis, we established an intervention model by giving 100 or 300 mg/kg metformin to mice after silica-instillation for 28 days. We continued the treatment for two weeks and observed a 100% survival rate in the treatment group (Fig. 1A). Representative H&E staining showed fibrotic remodeling characteristics by accumulating typical fibrotic nodules and abnormal alveolar structure in the silica group. Notably, metformin (100 or 300 mg/kg) intervention gradually attenuated severe histological changes (Fig. 1B). Moreover, metformin also reduced the degree of severity and distribution of lung lesions in silica-treated mice (Table 1). Consistently, the elevated expression of fibrotic markers (including α -SMA, Collagen I, Fibronectin, etc.) was significantly decreased in a metformin dose-dependent manner (Fig. 1C). The qRT-PCR results indicated that metformin also reduced the mRNA level of inflammation marker (TNF- α and IL- β) in the lung tissues compared with the silica group (Supplementary Fig. S1A and B). The collagen deposition levels were also observed in metformin intervention groups through hydroxyproline assay and indicated that metformin inhibited silica-induced the content of collagen deposition (Fig. 1D).

Next, we investigated the role of metformin (300 mg/kg was chosen) in the early fibrotic stage. The early-stage therapeutic effect of metformin was applied in mice following silica administration. Mice were treated with metformin or saline from day 2 to day 28, then collected lung tissues for the following analysis on day 28 (Fig. 2A). Administration of metformin in the early stage significantly alleviated silica-induced pulmonary injury and fibrosis as illustrated by the H&E staining of lung histopathological sections (Fig. 2B). Similarly, mice pretreatment with metformin displayed a significant decrease of fibrotic markers (α -SMA, Collagen I, Fibronectin) and epithelial-mesenchymal transition marker, vimentin (Fig. 2C and Supplementary Fig. S2A), coupled with lower content of hydroxyproline in the lung tissues (Fig. 2D). Of note, much lower levels of inflammation marker, TNF- α and IL-1 β , were detected in the metformin intervention group compared to the silica group (Supplementary Fig. S2B and C). Collectively, our results supported that metformin could be an effective therapy against silica-induced lung fibrosis in different stages of fibrotic.

Metformin attenuates SiO₂-induced cell cytotoxicity.

To further investigate the potential role of metformin in vitro, the cell cytotoxicity assay was performed to explore the optimal dose and time of silica and metformin. As shown in Fig. 3A, D, and supplementary

Fig. S3A, the cell viability of HBE, A549, and THP-1 were gradually suppressed under the treatment of different concentrations of silica. Besides, the cytotoxicity of cells also has a time-dependent occurrence (Fig. 3B and E). The viability results suggested that the 200 $\mu\text{g/ml}$ SiO_2 24 h treatment (cell viability decreased about 50%) showed moderate efficiency in HBE and A549 cells. This time dose was used in the rest of the experiments. As expected, co-treatment with various doses of metformin could inhibit HBE, A549 and THP-1 cells' cytotoxicity induced by SiO_2 (Fig. 3C and F and Supplementary Fig. S3B).

Increased apoptosis was accompanied by the induction of SiO_2 [31]. JC-1 staining showed that SiO_2 induced epithelium cell apoptosis by depolarizing the mitochondrial membrane potential. However, co-treatment with metformin significantly reversed the disruption of mitochondrial membrane potential (Fig. 3G and Supplementary Fig. S3C). Next, we used LDH release assay to investigate the viability of cells. Incubation of cells with SiO_2 resulted in an apparent increase in LDH release; conversely, the presence of metformin significantly reduced LDH leakage (Fig. 3H). Together, these results suggested metformin protected cells from SiO_2 -induced cytotoxicity.

Metformin inhibits SiO_2 -induced oxidative stress.

The generation of ROS is an essential indicator of oxidative stress and plays an important role in pulmonary fibrosis[32]. To examine the ROS generation in SiO_2 -treated cells, we used a DCFH-DA probe to detect cellular ROS production. As shown in Fig. 4A-C, the ROS generation was elevated after treatment with SiO_2 (A549 and HBE cells for 24h; THP-1 cells for 12h) compared to controls, and this elevation was inhibited by co-treatment with metformin.

Glutathione (GSH) is one of the major antioxidant guardians in cellular, which could exert a critical role in reducing oxidative stress levels[33]. To further explore the antioxidant ability of metformin, the oxidative damage in cells induced by SiO_2 was measured. The antioxidant activities of GSH were decreased (Fig. 4D), whereas the lipid peroxidation levels of MDA were increased after SiO_2 treatment (Fig. 4E). In contrast, treatment of metformin significantly enhanced GSH and decreased MDA content compared with the SiO_2 treatment group. Therefore, it appears that metformin may inhibit SiO_2 -induced oxidative stress in vitro.

Metformin inhibits SiO_2 -induced pulmonary macrophage inflammatory response.

It has been shown that macrophages, and inflammatory mediators, including IL-1 β and TNF- α , could contribute to exacerbating lung fibrosis[34]. Thus, we detected the levels of inflammatory mediators in silica-stimulated macrophages by qRT-PCR analysis. The results showed that the mRNA levels of IL-1 β and TNF- α were upregulated in a dose- (Fig. 5A and B) and time- (Fig. 5D and E) dependent manner. Besides, the western blot assay showed that the protein levels of IL-1 β and TNF- α were also increased in SiO_2 -treated macrophages (Fig. 5C). Following metformin co-treatment, the mRNA (Fig. 5F and G) and protein (Fig. 5H and Supplementary Fig. S4A) levels of IL-1 β and TNF- α were significantly decreased compared with the SiO_2 -stimulated group. All the data indicate that metformin could be an effective therapy for SiO_2 -induced pulmonary macrophage inflammation.

Metformin suppresses the SiO₂-induced EMT process in lung epithelial cells.

Next, we explored the appropriate dosage for SiO₂ stimulation in A549 and HBE cells. Western blot results showed that the expression of α -SMA and vimentin were increased, while E-cadherin expression decreased in a dose-dependent manner (Fig. 6A and Supplementary Fig. S5A, B), which indicated that the cell went through the EMT process. Meanwhile, metformin could enhance E-cadherin and down-regulated vimentin at protein (Fig. 6B and Supplementary Fig. S5C, D) and mRNA levels (Fig. 6C). TGF- β 1 is one of the main inducers of EMT and plays an essential role in lung fibrosis[35, 36]. In this study, we found that metformin also decreased the expression of TGF- β 1 induced by SiO₂ (Fig. 6D and Supplementary Fig. S5E). Subsequently, the wound-healing assay was carried out to detect the migration ability of cells, which showed that the migration ability of A549 and HBE cells was increased in the presence of SiO₂, while decreased in the intervention of metformin with a dose-dependent way (Fig. 6E and Supplementary Fig. S5F). These data suggested that metformin could suppress the process of EMT in epithelial cells induced by SiO₂.

Metformin inhibits the TGF- β 1-induced FMT process in pulmonary fibroblasts.

Fibroblast-myofibroblast transition (FMT) is an essential pathological feature during pulmonary fibrosis, and FMT-derived myofibroblasts are the primary source of ECM components[37, 38]. Importantly, TGF- β 1-induced FMT is the primary mechanism of fibrotic diseases.

To explore the role of metformin on TGF- β 1-stimulated FMT responses, we cultured MRC-5 cells with the presence of TGF- β 1 to establish a cell FMT model. The western bolt results showed that TGF- β 1 dose-dependently increased the levels of fibrotic markers including Fibronectin, Collagen I and α -SMA (Fig. 7A and Supplementary Fig. S6A). And it was also found that metformin could reverse the expression of fibrotic markers upregulated by TGF- β 1 (Fig. 7B, C and Supplementary Fig. S6B). The wound-healing assay showed that the migration of fibroblast cells induced by TGF- β 1 was reversed by metformin (Fig. 7D). Overall, our results demonstrated that metformin could modulate the FMT process stimulated by TGF- β 1 in fibroblast cells.

Metformin protects against SiO₂-induced lung fibrosis dependent on the AMPK pathway.

To determine whether metformin plays its protective role in an AMPK-dependent manner, cells were treated with AMPK inhibitor Compound C. The effects of metformin in the process of EMT, FMT, and inflammation responses were reversed by Compound C (Fig. 8A-C and Supplementary Fig. S7A, B). After metformin treatment, co-treatment with Compound C could reverse the EMT-blockage role of metformin (Fig. 8D, E and Supplementary Fig. S7C). Moreover, treatment with metformin significantly reduced TGF- β 1-induced the expression of α -SMA in MRC-5 cells, which was also reversed by Compound C (Fig. 8F and Supplementary Fig. S7D). Similarly, after metformin treatment, the mRNA expression of vimentin, as well as E-cadherin, was also reversed by Compound C (Fig. 8G, H). Taken together, these data indicated that metformin affects SiO₂-induced pulmonary fibrosis in an AMPK dependent manner.

Discussion

Silicosis is one of the potentially fatal lung diseases, mainly caused by long-term inhalation of respirable crystalline free silica (SiO_2) in occupational environments[39]. The essential characters of silicosis include the chronic inflammation response, and the continuous aggravation of the fibrotic process, eventually leading to respiratory failure[40]. Although attempts to prevent silicosis have been made for several decades, it remains a severe public health problem worldwide, especially in developing countries[41]. Currently, effective clinical therapies are limited. Few drugs can reverse the progression of silicosis. Even though lung transplantation is an effective intervention shown to provide the longest survival time, it is associated with the low availability of suitable lung donors and disease-specific challenges[42]. It is urgent to identify useful drugs to attenuate the development of silicosis. Hence, in this study, we established metformin intervention models *in vitro* and *in vivo* to explore its potential anti-fibrotic effects.

Metformin, a widely used miracle drug, is well known for treating type 2 diabetes. However, with advances in epidemiological and experimental researches, growing evidence suggests that metformin has multiple benefits in various diseases, including fibrotic diseases[43-45]. For example, metformin was found to alter the fate of myofibroblasts by inducing lipogenic differentiation and inhibit TGF- β 1-stimulated myogenic differentiation[46]. Besides, recent studies have shown that metformin could prevent age-associated ovarian fibrosis and exert anti-ovarian cancer effects[47]. Moreover, abundant data have indicated that metformin might attenuate PM2.5-induced lung injury and cardiac fibrosis[48]. Thus, these findings supported that metformin acted as a potential anti-fibrotic drug. In the present study, the positive effect of metformin was further investigated in the silica-induced fibrosis mouse model.

The inhalation of respiratory silica dust can induce inflammatory responses, the secretion of inflammatory factors, and high ROS levels, which contribute to chronic lung injury.[31] Importantly, the overproduction of intracellular ROS promotes the activation of alveolar macrophages and the secretion of pro-inflammatory cytokines, which aggravates lung dysfunction[49]. In this study, we found that SiO_2 exposure significantly increased the level of intracellular ROS, which was effectively attenuated after the metformin treatment. Moreover, SiO_2 treatment increased macrophage's IL-1 β and TNF- α levels, which were associated with the severity of lung inflammation. Similarly, other studies have also elucidated the antioxidative and anti-inflammatory properties of metformin in different experimental models[50-52]. For example, metformin attenuates hypoxia-induced mitochondrial ROS in different cell lines by modulating the HIF-1 α pathway[53]. Metformin also prevents ischemia-reperfusion induced inflammatory response in intestinal by TXNIP-NLRP3-GSDMD-dependent manner[54]. Additionally, the finding that metformin reversed SiO_2 -induced levels of GSH, MDA and inflammatory cytokines suggested that metformin could act as a useful antioxidant and anti-inflammatory agent.

Numerous studies have demonstrated that the contribution of EMT in fibrosis diseases, including pulmonary fibrosis[55]. Usually, EMT was one of the major sources of fibroblasts in various tissues. To evaluate the potential role of EMT in silicosis, our previous studies established a co-culture system by

culturing SiO₂ stimulated-epithelial cells with fibroblasts[56]. In the present study, we found that metformin upregulated E-cadherin level and downregulated the level of vimentin induced by SiO₂. Therefore, these results indicated that metformin acts as an effective medicine by halting the progression of EMT. Notably, the inhibitor of metformin, Compound C, could reverse the metformin-blocked EMT process. Also, metformin is involved in a variety of diseases by regulating the process of EMT. For example, metformin decreases cell invasion, growth, and EMT via modulation of miR-381/YAP activity in non-small cell lung cancer[57]. Metformin also suppressed DPP-4 inhibitor-induced EMT via the suppression of mTOR signaling in breast cancer[58].

The aberrant activation of fibroblast associated with excessive extracellular matrix accumulation is the main characteristic of pulmonary fibrosis[59]. In this study, we found that the treatment of metformin significantly inhibited TGF- β 1-induced myofibroblast differentiation. And, metformin regulated TGF- β 1-induced fibrotic markers expression at protein and mRNA level, which was reversed by Compound C. Hence, we speculated that metformin-mediated AMPK activation could inhibit the process of TGF- β 1-induced myofibroblast differentiation. Besides, it has been reported that metformin could reduce TGF- β 1-treated ECM protein accumulation in nasal polys-derived fibroblasts[60].

Growing evidence has identified that metformin exerts its pathology and physiology functions via both AMPK-dependent and AMPK-independent pathways. However, we only researched metformin to attenuate silica-induced lung fibrosis through AMPK-dependent molecular pathways. Further study is needed to focus on the independence of the AMPK pathways of metformin in our work.

Conclusions

Our finding indicated that metformin, dependent on AMPK signaling, attenuated silica-induced pulmonary fibrosis by decreasing cell toxicity, inflammation, oxidative stress, EMT, and fibroblast activation processes (Fig. 9). These results suggest that metformin administration is a potential therapy in fibrotic relative diseases.

Abbreviations

SiO₂, silicon dioxide; TGF- β 1, transforming growth factor beta 1; EMT, epithelial-mesenchymal transition; FMT, fibroblast-to-myofibroblast transition; ECM, extracellular matrix; TNF- α , tumor necrosis factor-alpha; IL-1 β , interleukin-1 beta; LDH, lactate dehydrogenase;

Declarations

Acknowledgments and funding

This project was supported by grants from the National Natural Science Foundation of China (82073518), and the Priority Academic Program Development of Jiangsu Higher Education Institutions (PAPD).

Authors' contributions

CD conceived the idea, CD, XQ and WY investigated the literature, CD, LG and SW participated the methodology; CD drafted the manuscript with the help of MD and ZS, HL and NC reviewed the manuscript. All authors read and approved the final manuscript.

Ethics statement

C57BL/6 mice (male, 5-6 weeks of mean age) were purchased from the Animal Center of Nanjing Medical University. All the animal experiments were conducted according to human-animal care standards and the claim of the Nanjing Medical University Ethics Committee (Nanjing, China).

Consent for publication

All the authors give consent.

Declaration of Competing Interest

The authors declare that they have no known competing financial interests.

Author details

^aDepartment of Occupational Medical and Environmental Health, Key Laboratory of Modern Toxicology of Ministry of Education, Center for Global Health, School of Public Health, Nanjing Medical University, Nanjing, 211166, China. chninjmu@126.com

^bInstitute of Occupational Disease Prevention, Jiangsu Provincial Center for Disease Control and Prevention, Nanjing 210028, China. hanlei@jscdc.cn

* Co-corresponding authors.

¹ These authors contributed equally to this work and should be considered co-first authors.

References

- [1] Z. Cao et al., "A novel pathophysiological classification of silicosis models provides some new insights into the progression of the disease," *Ecotoxicol Environ Saf*, vol. 202, p. 110834, Oct 1 2020.
- [2] Y. Qi, A. Zhao, P. Yang, L. Jin, and C. Hao, "miR-34a-5p Attenuates EMT through targeting SMAD4 in silica-induced pulmonary fibrosis," *J Cell Mol Med*, vol. 24, no. 20, pp. 12219-12224, Oct 2020.
- [3] F. Feng et al., "The Protective Role of Tanshinone IIA in Silicosis Rat Model via TGF-beta1/Smad Signaling Suppression, NOX4 Inhibition and Nrf2/ARE Signaling Activation," *Drug Des Devel Ther*, vol. 13, pp. 4275-4290, 2019.

- [4] R. Hoy and D. C. Chambers, "Silicosis: An ancient disease in need of a dose of modern medicine," *Respirology*, vol. 25, no. 5, pp. 464-465, May 2020.
- [5] L. Wollin et al., "Potential of nintedanib in treatment of progressive fibrosing interstitial lung diseases," *Eur Respir J*, vol. 54, no. 3, Sep 2019.
- [6] S. Fang et al., "circHECTD1 promotes the silica-induced pulmonary endothelial-mesenchymal transition via HECTD1," *Cell Death Dis*, vol. 9, no. 3, p. 396, Mar 14 2018.
- [7] Y. Li et al., "M10 peptide attenuates silica-induced pulmonary fibrosis by inhibiting Smad2 phosphorylation," *Toxicol Appl Pharmacol*, vol. 376, pp. 46-57, Aug 1 2019.
- [8] C. Zhang et al., "YY1 mediates TGF-beta1-induced EMT and pro-fibrogenesis in alveolar epithelial cells," *Respir Res*, vol. 20, no. 1, p. 249, Nov 8 2019.
- [9] X. Li et al., "Antifibrotic Mechanism of Cinobufagin in Bleomycin-Induced Pulmonary Fibrosis in Mice," *Front Pharmacol*, vol. 10, p. 1021, 2019.
- [10] Y. C. Chen et al., "Particulate matters increase epithelial-mesenchymal transition and lung fibrosis through the ETS-1/NF-kappaB-dependent pathway in lung epithelial cells," *Part Fibre Toxicol*, vol. 17, no. 1, p. 41, Aug 14 2020.
- [11] H. Cui et al., "Monocyte-derived alveolar macrophage apolipoprotein E participates in pulmonary fibrosis resolution," *JCI Insight*, vol. 5, no. 5, Mar 12 2020.
- [12] Z. Abassi, Y. Knaney, T. Karram, and S. N. Heyman, "The Lung Macrophage in SARS-CoV-2 Infection: A Friend or a Foe?," *Front Immunol*, vol. 11, p. 1312, 2020.
- [13] R. Gao et al., "Macrophage-derived netrin-1 drives adrenergic nerve-associated lung fibrosis," *J Clin Invest*, vol. 131, no. 1, Jan 4 2021.
- [14] S. Du et al., "Dioscin Alleviates Crystalline Silica-Induced Pulmonary Inflammation and Fibrosis through Promoting Alveolar Macrophage Autophagy," *Theranostics*, vol. 9, no. 7, pp. 1878-1892, 2019.
- [15] T. Xu et al., "MiR-326 Inhibits Inflammation and Promotes Autophagy in Silica-Induced Pulmonary Fibrosis through Targeting TNFSF14 and PTBP1," *Chem Res Toxicol*, vol. 32, no. 11, pp. 2192-2203, Nov 18 2019.
- [16] Y. Takenouchi, K. Kitakaze, K. Tsuboi, and Y. Okamoto, "Growth differentiation factor 15 facilitates lung fibrosis by activating macrophages and fibroblasts," *Exp Cell Res*, vol. 391, no. 2, p. 112010, Jun 15 2020.
- [17] S. Lin et al., "LncRNA Hoxaas3 promotes lung fibroblast activation and fibrosis by targeting miR-450b-5p to regulate Runx1," *Cell Death Dis*, vol. 11, no. 8, p. 706, Aug 26 2020.

- [18] S. G. Jang, J. Lee, S. M. Hong, S. K. Kwok, M. L. Cho, and S. H. Park, "Metformin enhances the immunomodulatory potential of adipose-derived mesenchymal stem cells through STAT1 in an animal model of lupus," *Rheumatology (Oxford)*, vol. 59, no. 6, pp. 1426-1438, Jun 1 2020.
- [19] J. Li et al., "Metformin limits osteoarthritis development and progression through activation of AMPK signalling," *Ann Rheum Dis*, vol. 79, no. 5, pp. 635-645, May 2020.
- [20] J. Liu et al., "Metformin suppresses proliferation and invasion of drug-resistant breast cancer cells by activation of the Hippo pathway," *J Cell Mol Med*, vol. 24, no. 10, pp. 5786-5796, May 2020.
- [21] A. R. Bland, N. Shrestha, R. L. Bower, R. J. Rosengren, and J. C. Ashton, "The effect of metformin in EML4-ALK+ lung cancer alone and in combination with crizotinib in cell and rodent models," *Biochem Pharmacol*, vol. 183, p. 114345, Jan 2021.
- [22] M. Jalali et al., "The effects of metformin administration on liver enzymes and body composition in non-diabetic patients with non-alcoholic fatty liver disease and/or non-alcoholic steatohepatitis: An up-to date systematic review and meta-analysis of randomized controlled trials," *Pharmacol Res*, vol. 159, p. 104799, Sep 2020.
- [23] Y. Guo et al., "Metformin alleviates allergic airway inflammation and increases Treg cells in obese asthma," *J Cell Mol Med*, Jan 9 2021.
- [24] M. J. Crowley et al., "Clinical Outcomes of Metformin Use in Populations With Chronic Kidney Disease, Congestive Heart Failure, or Chronic Liver Disease: A Systematic Review," *Ann Intern Med*, vol. 166, no. 3, pp. 191-200, Feb 7 2017.
- [25] Z. Lv and Y. Guo, "Metformin and Its Benefits for Various Diseases," *Front Endocrinol (Lausanne)*, vol. 11, p. 191, 2020.
- [26] K. Maniar, V. Singh, A. Moideen, R. Bhattacharyya, A. Chakrabarti, and D. Banerjee, "Inhalational supplementation of metformin butyrate: A strategy for prevention and cure of various pulmonary disorders," *Biomed Pharmacother*, vol. 107, pp. 495-506, Nov 2018.
- [27] H. Xiao et al., "Metformin ameliorates bleomycin-induced pulmonary fibrosis in mice by suppressing IGF-1," *Am J Transl Res*, vol. 12, no. 3, pp. 940-949, 2020.
- [28] S. Rangarajan et al., "Metformin reverses established lung fibrosis in a bleomycin model," *Nat Med*, vol. 24, no. 8, pp. 1121-1127, Aug 2018.
- [29] E. H. van Kammen-Wijnmalen, H. D. ten Brink, D. Hendriks, and E. F. Drion, "Prevalence of pneumoconiosis in diabetic coal-miners. A preliminary report," *J Chronic Dis*, vol. 22, no. 8, pp. 609-15, Feb 1970.

- [30] D. Cheng et al., "Long noncoding RNA-SNHG20 promotes silica-induced pulmonary fibrosis by miR-490-3p/TGFBR1 axis," *Toxicology*, p. 152683, Jan 19 2021.
- [31] J. Ma et al., "A Positive Feed Forward Loop between Wnt/beta-Catenin and NOX4 Promotes Silicon Dioxide-Induced Epithelial-Mesenchymal Transition of Lung Epithelial Cells," *Oxid Med Cell Longev*, vol. 2020, p. 3404168, 2020.
- [32] J. L. Larson-Casey, C. He, and A. B. Carter, "Mitochondrial quality control in pulmonary fibrosis," *Redox Biol*, vol. 33, p. 101426, Jun 2020.
- [33] F. Silvagno, A. Vernone, and G. P. Pescarmona, "The Role of Glutathione in Protecting against the Severe Inflammatory Response Triggered by COVID-19," *Antioxidants (Basel)*, vol. 9, no. 7, Jul 16 2020.
- [34] P. T. Santana et al., "P2Y12 Receptor Antagonist Clopidogrel Attenuates Lung Inflammation Triggered by Silica Particles," *Front Pharmacol*, vol. 11, p. 301, 2020.
- [35] S. H. Lee, O. Kim, H. J. Kim, C. Hwangbo, and J. H. Lee, "Epigenetic regulation of TGF-beta-induced EMT by JMJD3/KDM6B histone H3K27 demethylase," *Oncogenesis*, vol. 10, no. 2, p. 17, Feb 26 2021.
- [36] Q. Chen et al., "TGF-beta1 promotes epithelial-to-mesenchymal transition and stemness of prostate cancer cells by inducing PCBP1 degradation and alternative splicing of CD44," *Cell Mol Life Sci*, vol. 78, no. 3, pp. 949-962, Feb 2021.
- [37] J. Wang et al., "Microcystin-LR ameliorates pulmonary fibrosis via modulating CD206(+) M2-like macrophage polarization," *Cell Death Dis*, vol. 11, no. 2, p. 136, Feb 19 2020.
- [38] J. X. Zhang et al., "circHIPK3 regulates lung fibroblast-to-myofibroblast transition by functioning as a competing endogenous RNA," *Cell Death Dis*, vol. 10, no. 3, p. 182, Feb 22 2019.
- [39] J. Pang et al., "Multi-omics study of silicosis reveals the potential therapeutic targets PGD2 and TXA2," *Theranostics*, vol. 11, no. 5, pp. 2381-2394, 2021.
- [40] D. Wang et al., "Comparison of Risk of Silicosis in Metal Mines and Pottery Factories: A 44-Year Cohort Study," *Chest*, vol. 158, no. 3, pp. 1050-1059, Sep 2020.
- [41] X. Gao et al., "Pulmonary Silicosis Alters MicroRNA Expression in Rat Lung and miR-411-3p Exerts Anti-fibrotic Effects by Inhibiting MRTF-A/SRF Signaling," *Mol Ther Nucleic Acids*, vol. 20, pp. 851-865, Jun 5 2020.
- [42] P. M. George, C. M. Patterson, A. K. Reed, and M. Thillai, "Lung transplantation for idiopathic pulmonary fibrosis," *Lancet Respir Med*, vol. 7, no. 3, pp. 271-282, Mar 2019.
- [43] C. Wang et al., "Metformin inhibits pancreatic cancer metastasis caused by SMAD4 deficiency and consequent HNF4G upregulation," *Protein Cell*, vol. 12, no. 2, pp. 128-144, Feb 2021.

- [44] H. Yi et al., "Metformin Attenuates Renal Fibrosis in a Mouse Model of Adenine-Induced Renal Injury Through Inhibiting TGF-beta1 Signaling Pathways," *Front Cell Dev Biol*, vol. 9, p. 603802, 2021.
- [45] H. Kim et al., "Metformin inhibits chronic kidney disease-induced DNA damage and senescence of mesenchymal stem cells," *Aging Cell*, vol. 20, no. 2, p. e13317, Feb 2021.
- [46] V. Kheirollahi et al., "Metformin induces lipogenic differentiation in myofibroblasts to reverse lung fibrosis," *Nat Commun*, vol. 10, no. 1, p. 2987, Jul 5 2019.
- [47] C. W. McCloskey et al., "Metformin Abrogates Age-Associated Ovarian Fibrosis," *Clin Cancer Res*, vol. 26, no. 3, pp. 632-642, Feb 1 2020.
- [48] J. Gao et al., "Metformin protects against PM2.5-induced lung injury and cardiac dysfunction independent of AMP-activated protein kinase alpha2," *Redox Biol*, vol. 28, p. 101345, Jan 2020.
- [49] S. Liu et al., "Fullerene nanoparticles: a promising candidate for the alleviation of silicosis-associated pulmonary inflammation," *Nanoscale*, vol. 12, no. 33, pp. 17470-17479, Aug 28 2020.
- [50] d. H. Donatienne, P. Danhier, H. Northshield, P. Isenborghs, B. F. Jordan, and B. Gallez, "A versatile EPR toolbox for the simultaneous measurement of oxygen consumption and superoxide production," *Redox Biol*, vol. 40, p. 101852, Apr 2021.
- [51] A. R. Cameron et al., "Anti-Inflammatory Effects of Metformin Irrespective of Diabetes Status," *Circ Res*, vol. 119, no. 5, pp. 652-65, Aug 19 2016.
- [52] Q. Fei et al., "Metformin protects against ischaemic myocardial injury by alleviating autophagy-ROS-NLRP3-mediated inflammatory response in macrophages," *J Mol Cell Cardiol*, vol. 145, pp. 1-13, Aug 2020.
- [53] A. R. Chowdhury, J. Zielonka, B. Kalyanaraman, R. C. Hartley, M. P. Murphy, and N. G. Avadhani, "Mitochondria-targeted paraquat and metformin mediate ROS production to induce multiple pathways of retrograde signaling: A dose-dependent phenomenon," *Redox Biol*, vol. 36, p. 101606, Sep 2020.
- [54] Y. Jia et al., "Metformin protects against intestinal ischemia-reperfusion injury and cell pyroptosis via TXNIP-NLRP3-GSDMD pathway," *Redox Biol*, vol. 32, p. 101534, May 2020.
- [55] Y. Wang et al., "Snail-mediated partial epithelial mesenchymal transition augments the differentiation of local lung myofibroblast," *Chemosphere*, vol. 267, p. 128870, Mar 2021.
- [56] Y. Liu et al., "Long non-coding RNA-ATB promotes EMT during silica-induced pulmonary fibrosis by competitively binding miR-200c," *Biochim Biophys Acta Mol Basis Dis*, vol. 1864, no. 2, pp. 420-431, Feb 2018.

- [57] D. Jin et al., "Metformin-repressed miR-381-YAP-snail axis activity disrupts NSCLC growth and metastasis," J Exp Clin Cancer Res, vol. 39, no. 1, p. 6, Jan 6 2020.
- [58] E. Kawakita et al., "Metformin Mitigates DPP-4 Inhibitor-Induced Breast Cancer Metastasis via Suppression of mTOR Signaling," Mol Cancer Res, vol. 19, no. 1, pp. 61-73, Jan 2021.
- [59] X. Pan et al., "Lysine-specific demethylase-1 regulates fibroblast activation in pulmonary fibrosis via TGF-beta1/Smad3 pathway," Pharmacol Res, vol. 152, p. 104592, Feb 2020.
- [60] I. H. Park et al., "Metformin reduces TGF-beta1-induced extracellular matrix production in nasal polyp-derived fibroblasts," Otolaryngol Head Neck Surg, vol. 150, no. 1, pp. 148-53, Jan 2014.

Tables

Table 1 Effect of Metformin administration on lung histopathology

Groups	Lesion severity grade					Average Severity grade	Lesion distribution grade					Average Distribution grade		
	0	1	2	3	4		5	0	1	2	3		4	5
Saline	6						----	6						----
Silica				1	2	3	4.33±0.33			1	1	3	1	3.67±0.42
Silica+ 100mg/kg Metformin		2			4		3.67±0.84		2	4				1.67±0.21 ^a
Silica+ 300mg/kg Metformin	1	3	1			1	1.67±0.71 ^a	1	4	1				1.00±0.26 ^a

Values represent the means ± SD of 6 for each group. ^a $p < 0.05$ vs. silica group (independent-sample t-test).

Figures

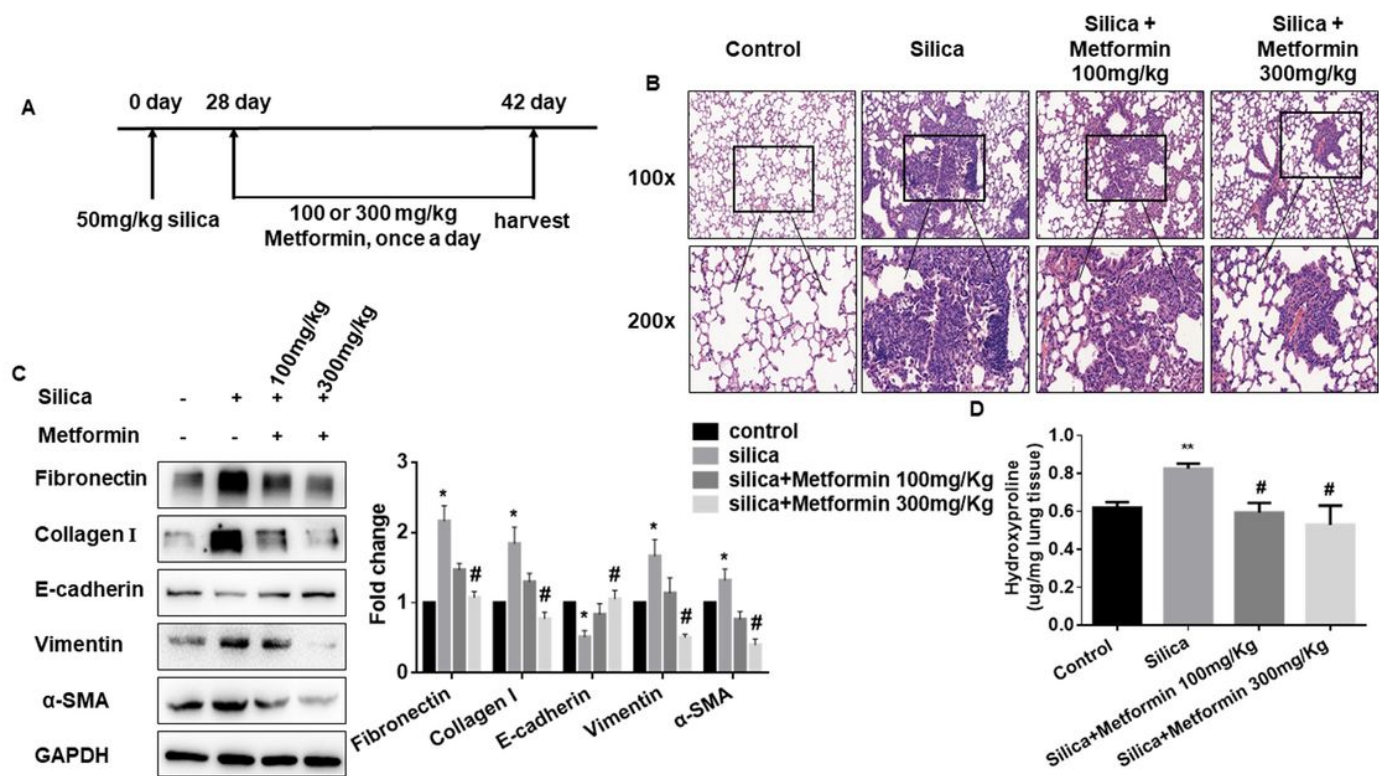


Figure 1

Metformin attenuates SiO₂-induced lung fibrosis in vivo. (A) Schematic diagram of the metformin treatment mouse model. (B) H&E staining reflected that the histological changes of lung tissues of different groups. (C) The protein levels of Fibronectin, Collagen I, E-cadherin, vimentin, and α -SMA in each group, with * $p < 0.05$ vs. control and # $p < 0.05$ vs. the silica group. (D) Hydroxyproline content of the lung tissues in each group was detected to measure collagen deposition, with ** $p < 0.01$ vs. control and # $p < 0.05$ vs. the silica group.

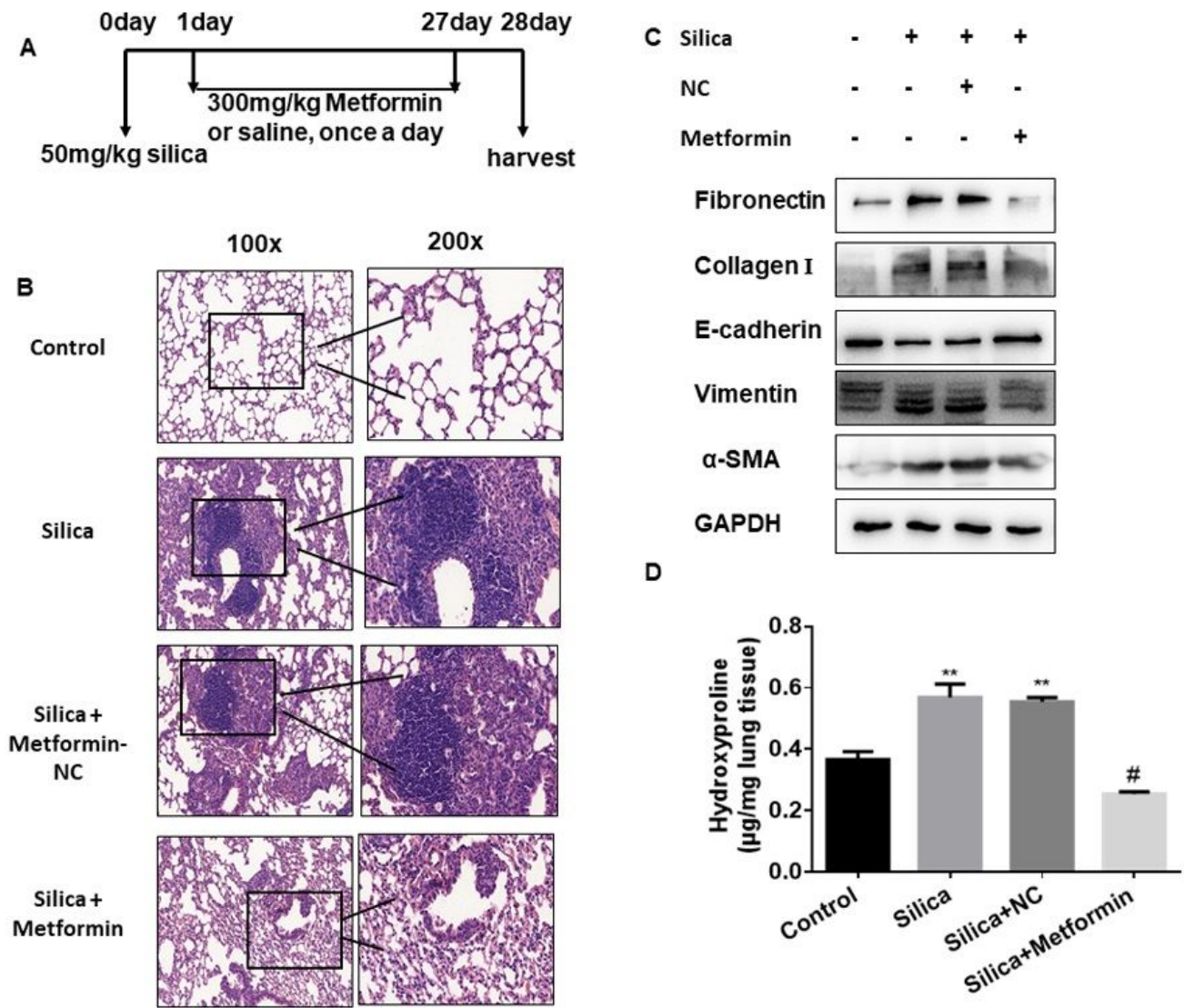


Figure 2

Metformin attenuates SiO₂-induced lung fibrosis in vivo. (A) Schematic diagram of metformin intervention in the silica-induced pulmonary fibrosis mouse model. (B) The histology of lung tissues was detected by H&E staining in different groups. (C) The protein levels of Fibronectin etc. in lung tissues via western blotting assay. (D) The collagen deposition of different groups was performed by hydroxyproline content assay, with ***p* < 0.01 vs. control and #*p* < 0.05 vs. the silica plus NC group.

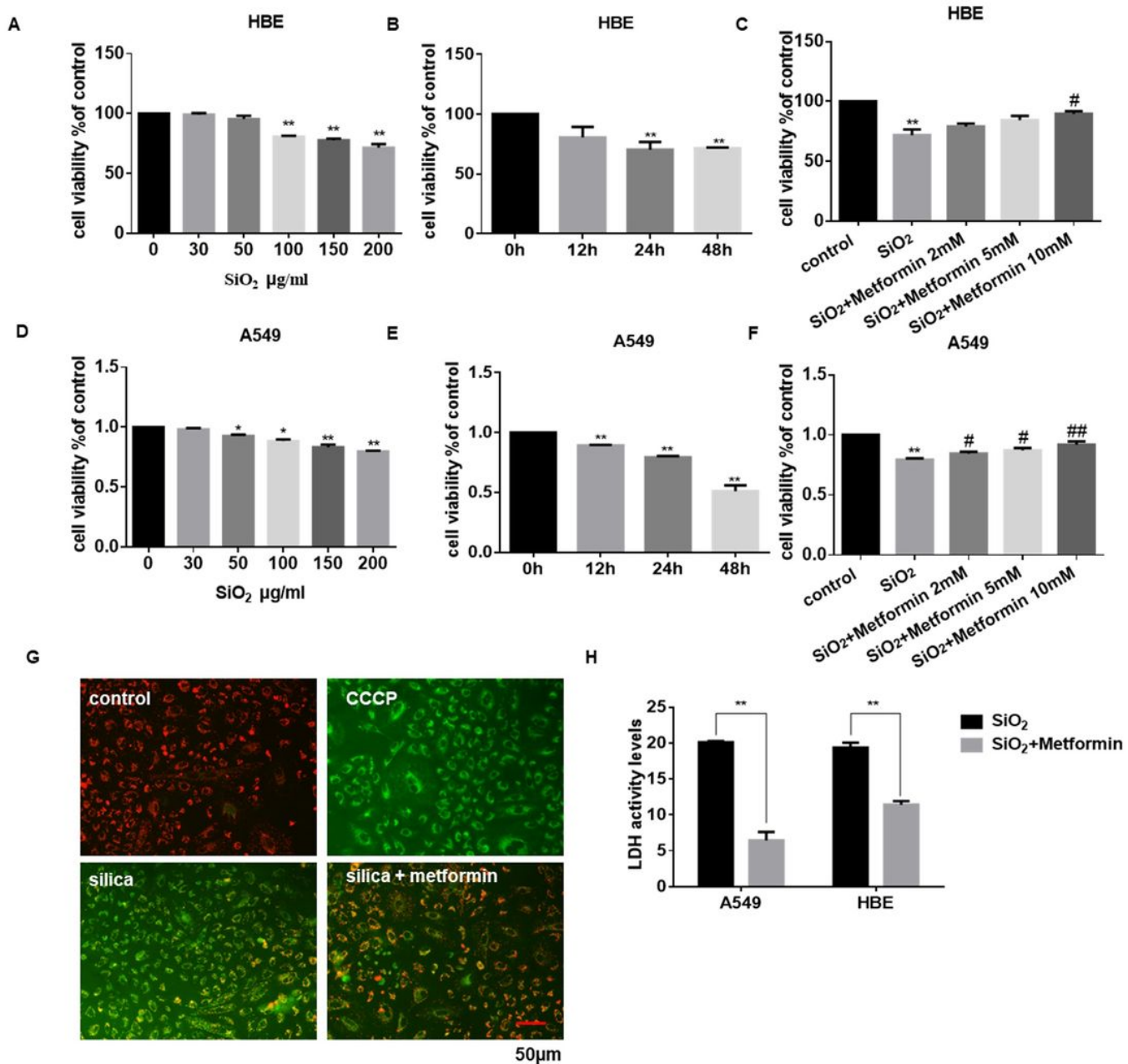


Figure 3

Metformin attenuates SiO₂-induced cell cytotoxicity. (A, B, D, E) Cell viability was detected by cck8 assay in HBE and A549 cells. HBE (A) and A549 (D) cells were treated for 24h in different concentrations of SiO₂ (0-200 $\mu\text{g/ml}$). HBE (B) and A549 (E) cells were cultured with 200 $\mu\text{g/ml}$ SiO₂ for 12, 24, and 48h separately. (C, F) HBE (C) and A549 (F) cells were incubated with 200 $\mu\text{g/ml}$ SiO₂ for 24h with or without metformin (2-10 mM/ml). After that, the cell viability was analyzed by cck8 assay. (G) The mitochondrial membrane potential of A549 cells was measured by JC-1 staining. CCCP: the positive control, Green fluorescence: the monomer, red fluorescence: the J-aggregates, scale bar = 50 μm . (H) LDH activity of the A549 and HBE cells was measured using LDH assay, with ** $p < 0.01$ vs. silica group.

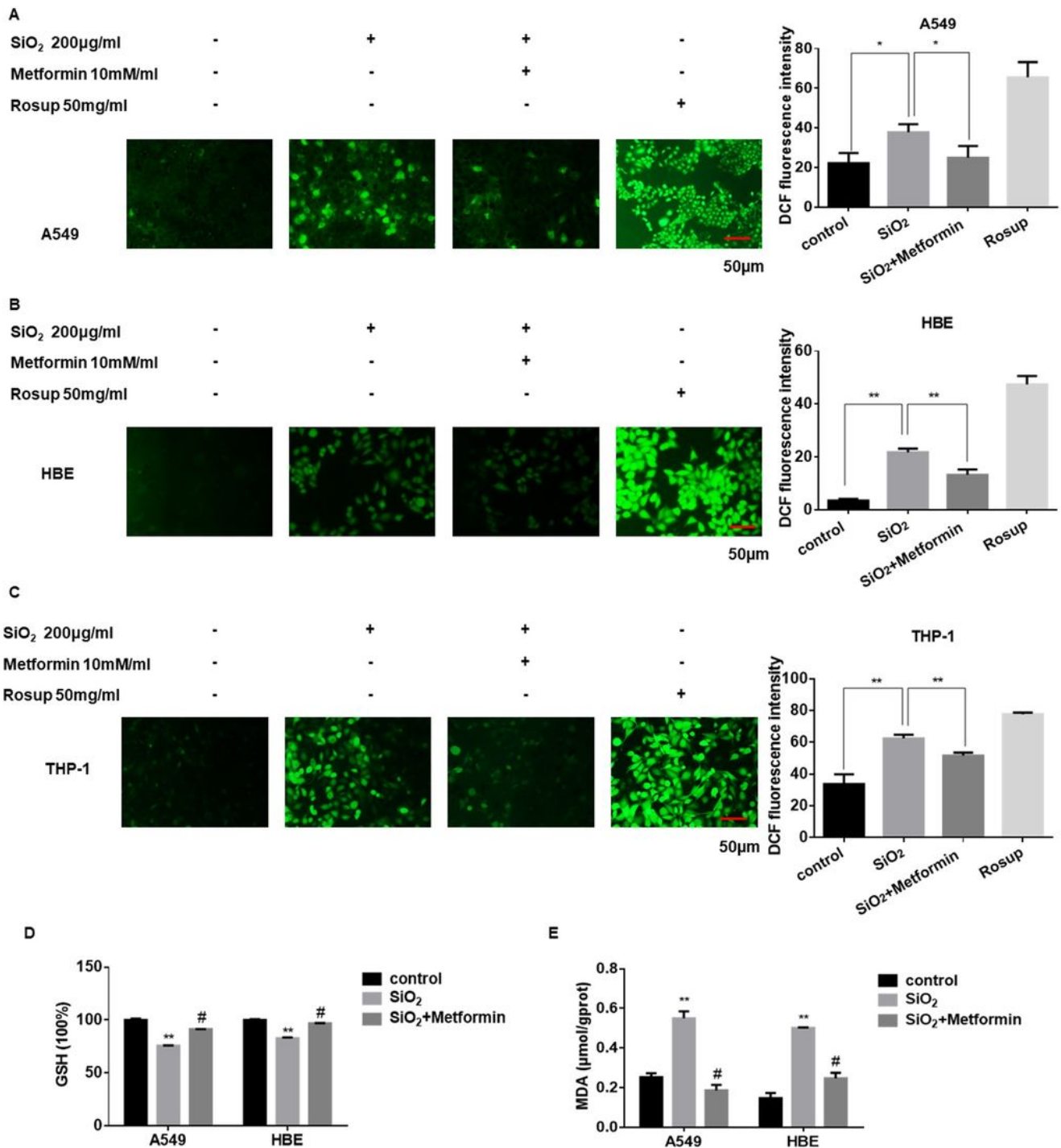


Figure 4

Metformin inhibits SiO₂-induced oxidative stress. (A-C) The intracellular ROS generation of A549 (A), HBE (B), and THP-1 (C) cells were determined by the DCFH-DA probe, respectively. With **p* < 0.05 and ***p* < 0.01 vs. control or silica group. (D-E) A549 and HBE cells were treated with silica and metformin for 24h. The levels of GSH (D) and MDA (E) were determined by commercial kits. With ***p* < 0.01 vs. control and #*p* < 0.05 vs. the silica group.

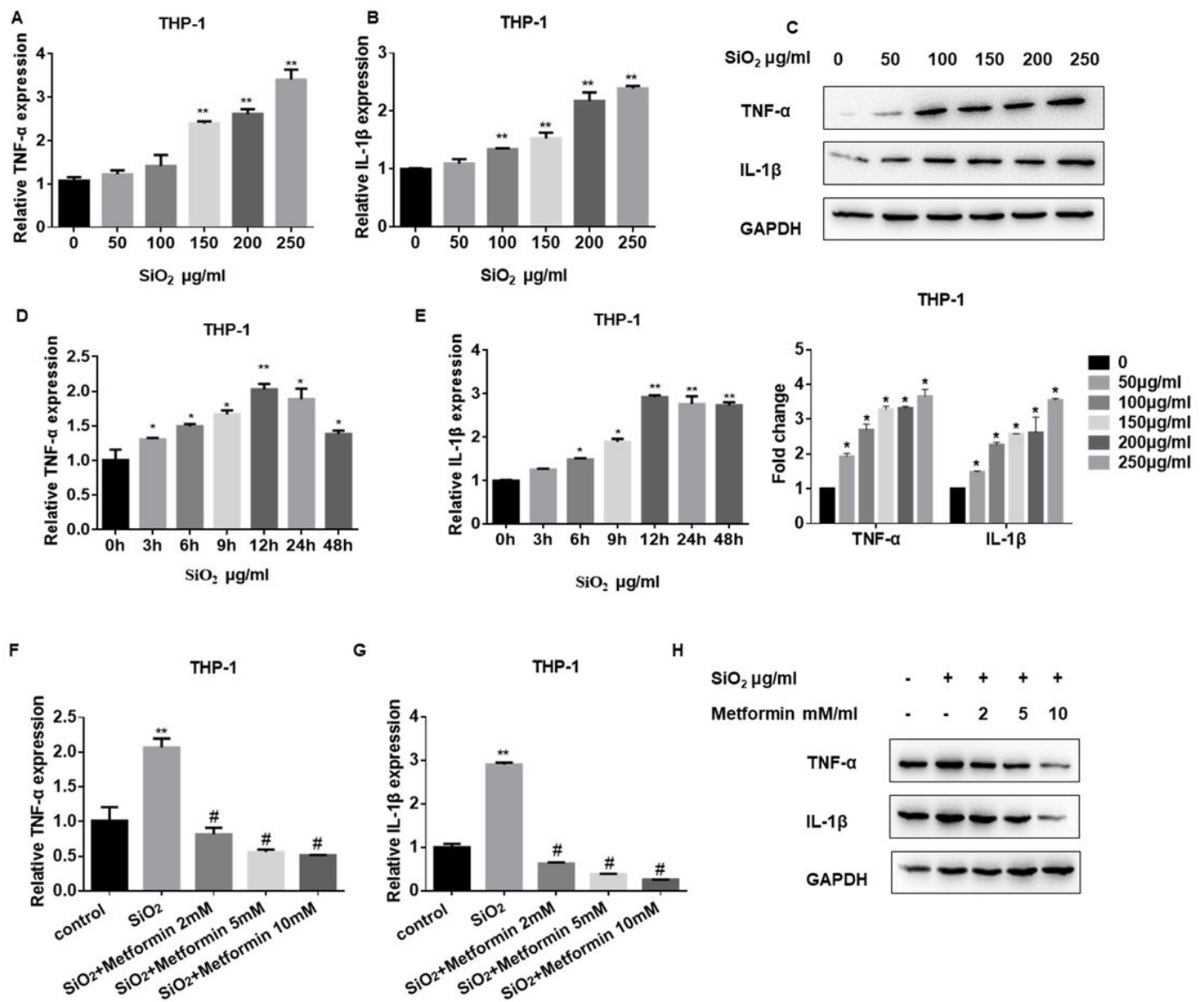


Figure 5

Metformin inhibits SiO₂-induced pulmonary macrophage inflammatory response. (A, B, D, E) qRT-PCR detection of TNF-α (A, D) and IL-1β (B, E) mRNA expression in THP-1 cells from different concentration SiO₂ and different time treatment, with **p* < 0.05 and ***p* < 0.01 vs. control group. (C) Western blots of TNF-α and IL-1β in THP-1 cells after incubated with SiO₂. (F, G) qRT-PCR detection of TNF-α (F) and IL-1β (G) mRNA expression in THP-1 cells after silica and metformin co-treatment for 12h, with ***p* < 0.01 vs. control and #*p* < 0.05 vs. the silica group. (H) Western blots of TNF-α and IL-1β in THP-1 cells after incubated with SiO₂ and metformin for 12h.

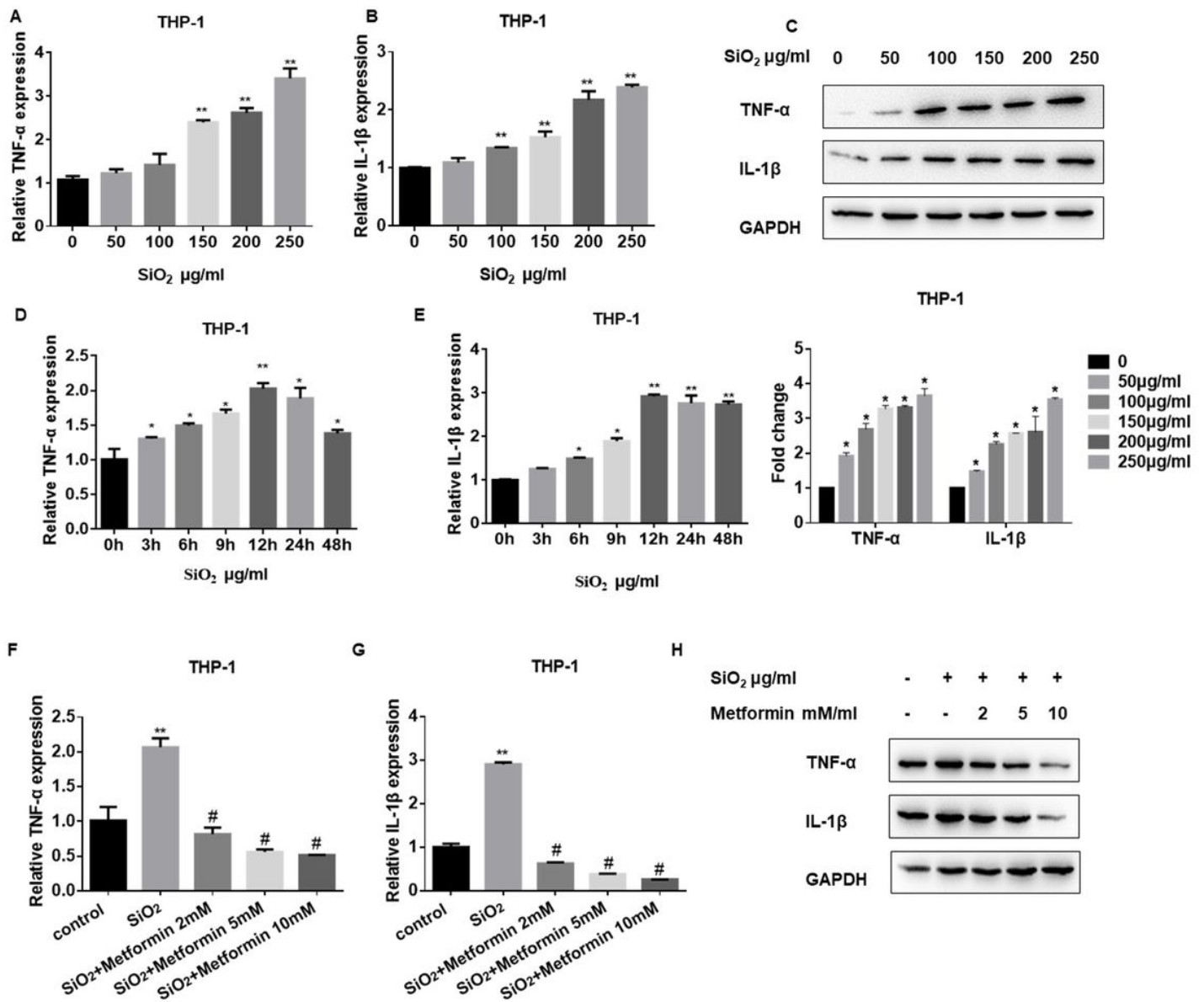


Figure 6

Metformin suppresses the SiO₂-induced EMT process in lung epithelial cells. (A) The protein levels of Fibronectin, E-cadherin, vimentin and α -SMA in different doses of silica treatment in A549 and HBE cells. (B) Western blotting showing Fibronectin, E-cadherin, vimentin and α -SMA protein levels with silica and metformin co-treatment in A549 and HBE cells. (C-D) qRT-PCR detection of E-cadherin, vimentin (C) and TGF- β 1 (D) mRNA expression in A549 cells after cultured with silica and different doses of metformin. With ** $p < 0.01$ vs. control and # $p < 0.05$ vs. the silica group. (E) Wound-healing assay and quantified wound gap of cell scratches detected the migration of A549 cells for the indicated groups, with * $p < 0.05$ vs. the silica group.

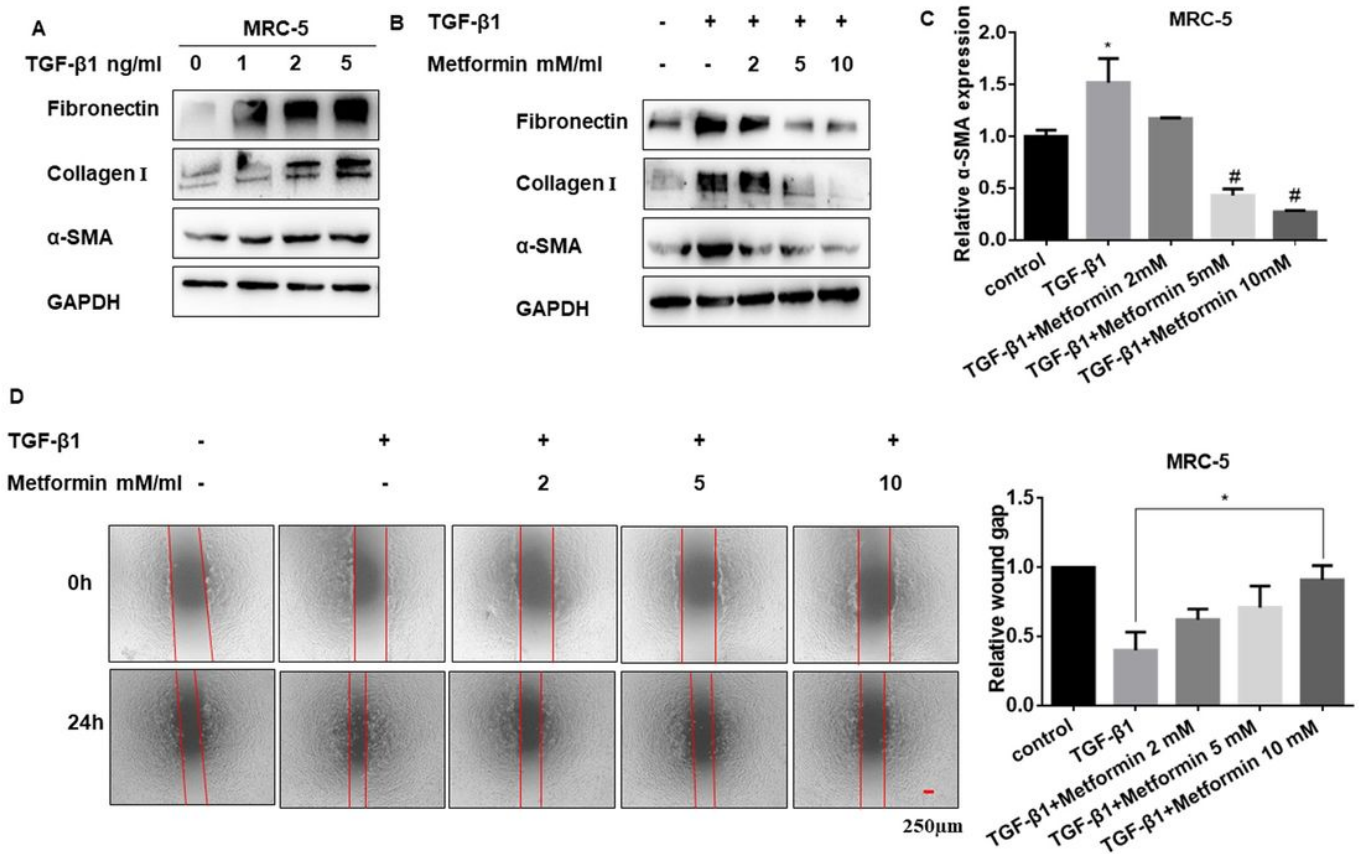


Figure 7

Metformin inhibits the TGF- β 1-stimulated FMT process in pulmonary fibroblasts. (A) The protein levels of Fibronectin, Collagen I and α -SMA in MRC-5 cells are treated by different doses of TGF- β 1. (B) Western blotting showing Fibronectin, Collagen I and α -SMA protein levels with TGF- β 1 and metformin co-treatment in MRC-5 cells. (C) qRT-PCR detection of α -SMA mRNA expression in MRC-5 cells after cultured with TGF- β 1 and different doses of metformin, with ** $p < 0.01$ vs. control and # $p < 0.05$ vs. the TGF- β 1 group. (D) Wound-healing assay and quantified wound gap of cell scratches detected the migration of MRC-5 cells for the indicated groups, with * $p < 0.05$ vs. the TGF- β 1 group.

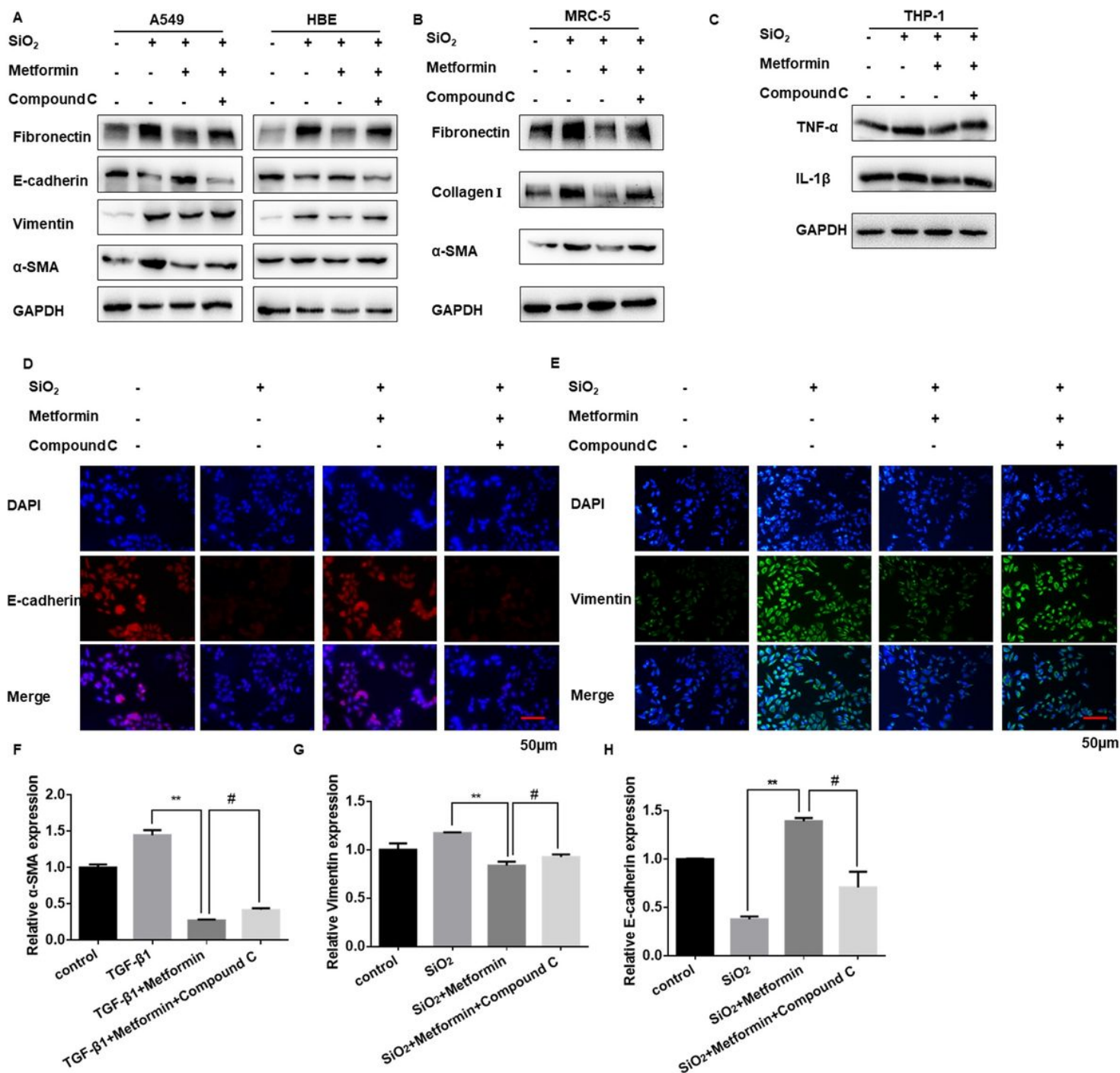


Figure 8

Metformin protects against SiO₂-induced lung fibrosis dependent on the AMPK pathway. (A) The protein levels of Fibronectin, E-cadherin, vimentin, and α-SMA in A549 and HBE cells treated by silica, silica plus metformin and silica, metformin plus compound C. (B) Western blotting showing Fibronectin, Collagen I and α-SMA protein levels with different treatment in MRC-5 cell. (C) The protein levels of TNF-α and IL-1β in THP-1 cells for indicated groups. (D, E) Immunofluorescence staining of E-cadherin (D) and vimentin (E) in HBE cells in different groups. E-cadherin stained red, vimentin stained green, DAPI was stained blue,

scale bar = 50 μm . (F-H) qRT-PCR detection of α -SMA (F), vimentin (G) and E-cadherin (H) mRNA expression for the indicated groups, with $**p < 0.01$ vs. TGF- β 1 or silica group and $\#p < 0.05$ vs. the TGF- β 1 or silica plus metformin group.

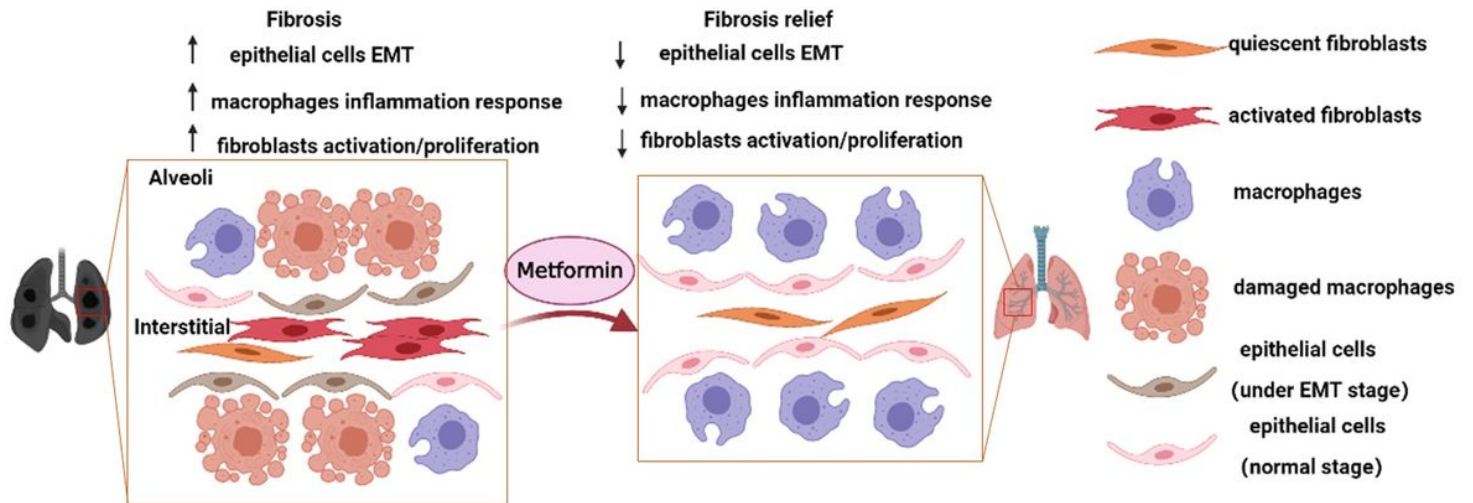


Figure 9

Schematic illustration represented the role of metformin in pulmonary fibrosis. Created with BioRender.com.

Supplementary Files

This is a list of supplementary files associated with this preprint. Click to download.

- [Fig.S7.tif](#)
- [Fig.S6.tif](#)
- [Fig.S5.tif](#)
- [Fig.S4.tif](#)
- [Fig.S3.tif](#)
- [Fig.S2.tif](#)
- [Fig.S1.tif](#)